



Electrical Conduction Mechanisms in Synthesized Ethylene Propylene Diene Monomer Rubber Loaded with High Abrasion Furnace Carbon Black

K Alfaramawi*, S Abboudy, L Abulnaser & A O Haridy

Department of Physics, Faculty of Science, Alexandria University, Alexandria 215 11, Egypt

Received 1 September 2021; accepted 5 October 2021

Ethylene Propylene Diene Monomer (EPDM) rubber filled with High Abrasion Furnace (HAF) carbon black at various concentrations (30, 40, 50, 80 phr) were synthesized and electrically characterized. The structure of the synthesized EPDM/HAF composites was studied by XRD and the surface morphology was analyzed by SEM. The XRD patterns revealed that the structure was partially amorphous with some crystalline phases. SEM micrographs showed a set of carbon black aggregates with different dimensions depending on the amount of carbon black filler. The electrical resistivity (conductivity) of the composites was investigated as a function of temperature and filler content. The electrical conductivity was greatly influenced by both the temperature and carbon black filler content. The conduction mechanisms were analyzed at different temperature regions. A variable range hopping process was suggested to explain the temperature dependence of the conductivity of low mass fraction carbon black. At higher carbon black concentration, the behavior of the conductivity is of a semiconductor-like and a metallic-like behavior. The concept of metal-insulator transition was suggested to explain the conductivity of the composites.

Keywords: EPDM rubber, HAF carbon black, Composites, Percolation, Resistivity, Aggregates, Variable range hopping, Metal-insulator transition

1 Introduction

Rubbers loaded with electrically conductive-based fillers have attracted great interest during the last decades due to their applications such as plastic batteries, sensors, electro-chromic displays, electromagnetic interference shielding, fuel cells, circuit boards *etc.*¹⁻⁵. When rubber is filled with conductive additives, such as carbon black, the electrical conductivity of the formed composite is enhanced. This is because the charge carriers can form a conductive path through the insulating matrix. The properties of the induced rubber-carbon black composite depend widely on the type and structure of both polymer and carbon black. The internal filler-filler interaction inside the composite is responsible for the formation of three-dimensional aggregation structures within the bulk of the rubber matrix⁶. The carriers can jump from one aggregate to another making their own conductive path. Many approaches were introduced to explain the behavior of the electrical conductivity in the conductive filler reinforced rubbers. Percolation theory⁷ was often used to analyze the filler concentration dependence of the electrical conductivity. On the other hand, the Fluctuation

Induced Tunneling (FIT) theory, proposed by Sheng & Klafter⁸, was commonly used to describe heterogeneous composites and its electrical conductivity.

Voet *et al.*⁹ discussed the conductivity of the composite on the basis of the possibility of non-ohmic conduction in the system. McCullough model¹⁰ was based on the use of transport phenomena for predicting conductivity of polymer composite. Scarisbrick¹¹ proposed a statistical model for a system consisting of conducting filler in a polymer matrix. It was assumed that all the conducting particles in the composite were randomly distributed spheres. The conductivity of the system was based on the probability of formation of conductive network through inter-particle contacts. El-Messieh *et al.*¹² reported that the aspect ratio and surface area to volume ratio of fillers play very important role in establishing a conductive network. Their analysis revealed that when the filler concentration is below the percolation threshold, the differences between the calculated and experimental conductivities were more pronounced. Reffae *et al.*¹³ studied the electrical and mechanical properties of acrylonitrile rubber (NBR), linear low-density polyethylene (LLDPE) and NBR/LLDPE blends before and after the addition of high abrasion furnace black (HAF) with different

*Corresponding author: (E-mail: kalfaramawi@alexu.edu.eg)

contents in order to find out the percolation thresholds in relation to the network formation.

In a recent work by Kolonelou *et al.*¹⁴, the electrical conductivity of Polyvinyl alcohol/polyvinylidene fluoride blends reinforced with low enough mass fraction of nano-graphene platelets (NGPs) was found to be comparable to that of a semiconductor. Zeid¹⁵ studied the effect of gamma radiation on the mechanical, thermal, and electrical properties of Ethylene Propylene Diene Monomer (EPDM)/NBR rubber blends loaded with HAF at room temperature. Effect of HAF carbon black on curing, mechanical, thermal, and neutron shielding properties of natural rubber-low-density polyethylene composites was studied by Sajith *et al.*¹⁶. They concluded that high percentage of HAF leads to a filler network formation in the composite. The study performed by Azizi *et al.*¹⁷ on EPDM and EPDM/Silicon rubber composites loaded with some additives showed an increase in the dielectric constant and AC dielectric breakdown strength. In addition, a significant increase in the thermal stability and thermal conductivity of this composite were noticed.

Dielectric, thermal, and water absorption properties of some EPDM/Flax fiber composites were studied by Airinei *et al.*¹⁸. A monotonic decrease of the dielectric constant and dielectric loss with the increase of frequency was recorded. However, at higher frequencies (above 10^3 Hz), independent behavior was observed. The increase of the dielectric constant and dielectric loss with the frequency was assumed to be due to the increase of the number of polar groups in the composites leading to a higher orientation polarization. A short review about the effect of carbon black and graphene on the performance of EPDM rubber composites was given by Mishra¹⁹. Mahmood *et al.*²⁰ studied the effect of nanocrystalline CaO particles on mechanical, thermal, and electrical properties of EPDM rubber. It was found that adding CaO nanocrystalline particles increases the thermal stability of the glass transition temperature, as well as the hardness of the EPDM rubber. Electrical properties of polymer blend composites based on Silicone rubber/EPDM/Clay hybrid for high voltage insulators were examined by Bazli *et al.*²¹. Jha *et al.*²² studied the morphology, barrier, and electrical properties (as a function of frequency) of Oil-extended EPDM/Nanographite nanocomposites.

Experimental and theoretical analyses on mechanical properties of hybrid Graphene/Graphene

oxide reinforced EPDM/NBR nanocomposites were discussed by Paran *et al.*²³. Both types of platelet-like nanoparticles were found to affect on the mechanical properties of this hybrid composite. Dielectric behavior of ternary polymer blend nanocomposites including EPDM, was discussed by Padhi *et al.*²⁴. The change in the dielectric behavior with frequency was attributed to a possible change in polarization and due to breaking of some aggregates at high temperatures.

In the present work, composites of EPDM rubber loaded with HAF carbon black were synthesized. The structure was analyzed by X-ray diffraction (XRD) and Scanning Electron Microscopy (SEM). The effect of various HAF carbon black concentrations on the electrical conductivity of the polymeric EPDM rubbers at different temperatures was studied. Thus, the electrical conductivity of the composites was examined as a function of both carbon black concentration and temperature. Conduction mechanisms at different temperature regions were specified. The new and novel trend in our composite system was the possibility of finding a metal-insulator transition in the electrical behavior which depends on the amount of carbon black content in the composite. This property can be used practically as switches and sensors.

2 Experimental Method

EPDM rubber was used as main matrix. HAF carbon black at 30, 40, 50, 80 and 100 part per hundred part of rubber by weight (phr) was used as a filler. The constituents were mixed according to the Compounds and Preparing Standard Vulcanized Sheets (ASTM D 3182)²⁵. The rubber and the additives (as indicated in Table 1) were mixed by using two roll mills of 300 mm length, 150 mm

Table 1 — Composition of EPDM rubber/HAF carbon black samples.

Ingredient (phr)*	Sample code				
	H30	H40	H50	H80	H100
EPDM rubber	100	100	100	100	100
Stearic acid	2	2	2	2	2
Zinc oxide	5	5	5	5	5
Diocetyl phthalate	50	50	50	50	50
HAF carbon black (N-330)	30	40	50	80	100
Volume fraction of the carbon black	0.2	0.25	0.294	0.4	0.455
Benzothiazyl Disulfide	1.5	1.5	1.5	1.5	1.5
Tetramethylthiuram Disulfide	2	2	2	2	2
Sulfur	3	3	3	3	3

* Part per hundred part of rubber by weight

diameter, speed of slow roll 18 rpm and 1.4 gear ratio. The rubber composite was left for 24 hours before vulcanization. The vulcanization process was carried out by using an electrically heated platen hydraulic press at 150 ± 2 °C and 15 MPa for 15 min. The compositions and sample coding were shown in Table 1.

Square-shaped sheets with a thickness of 1 mm were prepared to study the morphology of the composites. Additionally, bar-shaped samples of dimensions $1 \times 0.1 \times 0.2$ cm³ were prepared for electrical measurements. The direction of molding was recorded to be in the same direction of the bar-shaped samples through the vulcanization process where all electrical properties were in the longitudinal direction. Non-inductive electric oven was used to perform the electrical measurements at different temperatures. The samples were fixed between ground-shielded connections inside the electric oven.

The structure of the EPDM/HAF samples was analyzed by X-ray diffraction (XRD) at room temperature using a PANalytical X'Pert ProMPD-diffractometer (the Netherlands) operated at a voltage of 45 kV and current of 40 mA. It equipped with a Ni filter using CuK_α ($\lambda = 1.540$ Å) radiation in the 2θ range from 10° to 90° . The surface morphology of the composites was studied by Scanning Electron Microscopy (SEM) (type: JSM-IT200 SEM microscope). The electrical properties of the investigated samples were carried out in the temperature range from room temperature up to 400 K. Prema 6048 Integrating Digital Multimeter and handmade constant current source were employed.

3 Results and Discussion

3.1 Structural analysis

Figure 1 represents the XRD chart of samples H30, H40, H50, H80 and H100. All samples showed two broad peaks around $2\theta = 20^\circ$ and 45° , corresponding to interlayer spacings of 3.62 Å and 2.10 Å respectively (calculated from Bragg's equation). The appearance of these two peaks were assumed to be due to reflections from the HAF carbon black (002) and (100) planes respectively^{26,27}.

The formation of the carbon black in the rubber was discussed by Biscoe & Warren²⁸. The carbon black in the matrix is grown as small layers with the carbon atomic positions as graphite within the layers.

This means that the carbon black is dispersed in the amorphous rubber as collective particles on the shape of aggregates or as agglomerates. Therefore, in our case, the presence of such aggregates may improve the formation of crystal phase and lead to convert the structure of the composites to partially crystalline.

Moreover, inspection of Fig. 1 indicated that the peaks, generally, are shifted toward larger 2θ angle with the increase of the HAF carbon black concentration. This in accordance leads to an increase in the degree of crystallinity of the composites²⁹.

Fig. 1 also shows several small, sharp peaks at 2θ angles of approximately 31° , 33° , 36° , 38° , 44° , 56° and 64° , 77° and 82° . The presence of such peaks might be due to some residual, unreacted ZnO accelerator in the vulcanization process. This finding was recorded by many researchers in various rubber composite systems³⁰.

Figure 2 demonstrates the SEM photographs for samples H30, H40, H50, H80 and H100. Dispersion of the carbon black in the rubber matrix was

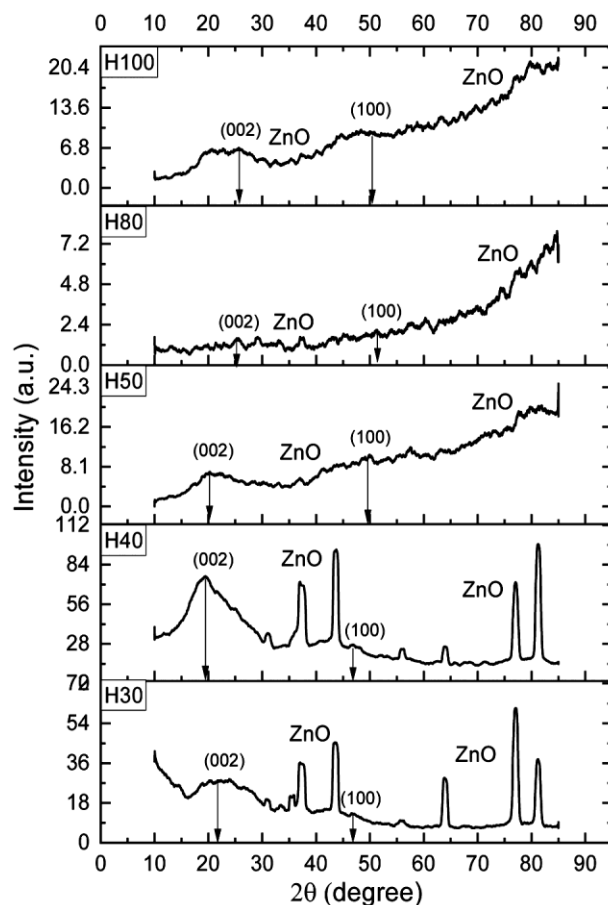


Fig. 1 — XRD chart for the EPDM/HAF composites with HAF carbon black loading content 30, 40, 50, 80 and 100 phr

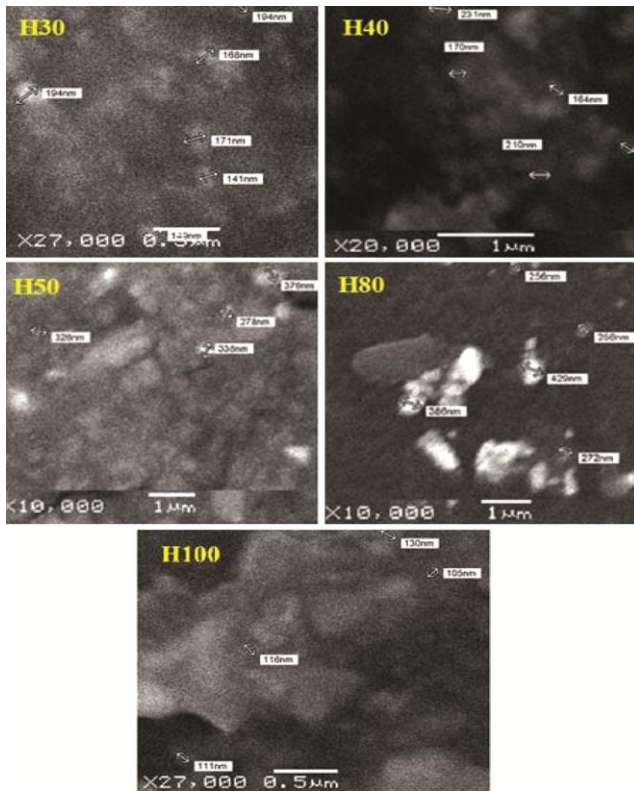


Fig. 2 — SEM photographs of EPDM/HAF samples H30, H40, H50, H80 and H100 with carbon black contents 30, 40, 50, 80 and 100 phr respectively.

observed. The filler distribution varied by the carbon black content. In H30 a small number of aggregates was noticed while in sample H100 large agglomerates were recorded. Estimation of smallest aggregate diameters revealed that in sample H30, the diameters were ranged between 140 to 190 nm. If the average diameter of one particle (HAF carbon black) is approximately 30 nm, then, at least 5 or 6 particles are collected to form one small aggregate in the matrix. For sample H40, the diameter of the smallest aggregates varied from 165 to 230 nm indicating that more HAF particles were gathered together. The same trend was recorded for samples H50, H80 and H100. Moreover, large aggregates were established with diameters exceed 400 nm in samples H80 and H100.

3.2 Electrical Properties

3.2.1 Filler concentration dependence of conductivity

Figure 3 depicts the electrical conductivity (σ) of the EPDM/HAF composites versus HAF filler volume fraction (ϕ) at three different temperatures: room temperature (295 K), 313 K and 323 K. The same trend of the conductivity was noticed at the three

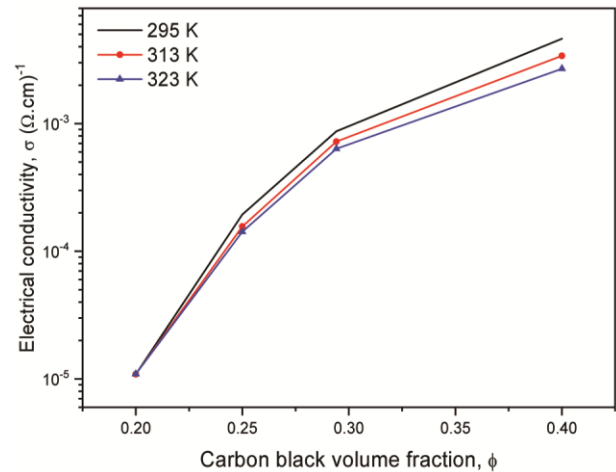


Fig. 3 — Electrical conductivity versus HAF carbon black volume fraction of EPDM/HAF composites at three temperatures 295 K, 313 K and 323 K

chosen temperatures. The conductivity increased monotonically with the filler volume fraction indicating the noticeable dependence of σ on the HAF filler concentration. This behavior may be described using the percolation approach at constant temperature⁷.

According to the percolation theory, the conductivity as a function of filler volume fraction is given by⁷:

$$\sigma = \sigma_o (\phi - \phi_c)^t \quad \dots (1)$$

where σ_o and ϕ_c are the conductivity and filler volume fraction at percolation threshold, respectively, and t is the conductivity exponent. The value of ϕ_c can be calculated from Janzen model³¹:

$$\phi_c = \frac{1}{1+4\rho_c DBP} \quad \dots (2)$$

where DBP is the Dibutyl-Phthalate absorption number of the carbon black filler and ρ_c its density. Substituting $\rho_c = 1.32 \text{ g/cm}^3$ and $DBP = 102 \text{ cm}^3/100\text{g}$ for HAF carbon black, one can estimate the value of ϕ_c as 0.16 for the investigated EPDM/HAF composites.

In order to examine the percolation behavior of the EPDM/HAF composites, $\ln \sigma$ versus $\ln(\phi - \phi_c)$ at 295 K, 313 K and 323 K was plotted (Fig. 4). Inspection of the figure revealed that the relations were almost straight lines. This satisfied equation (1) and therefore, it can confirm the presence of the percolation in the EPDM/HAF samples at this temperature range. From the slope of the straight lines in Fig. 4, values of the conductivity exponent t were calculated as 3.27 ± 0.27 , 3.62 ± 0.34 and $3.74 \pm$

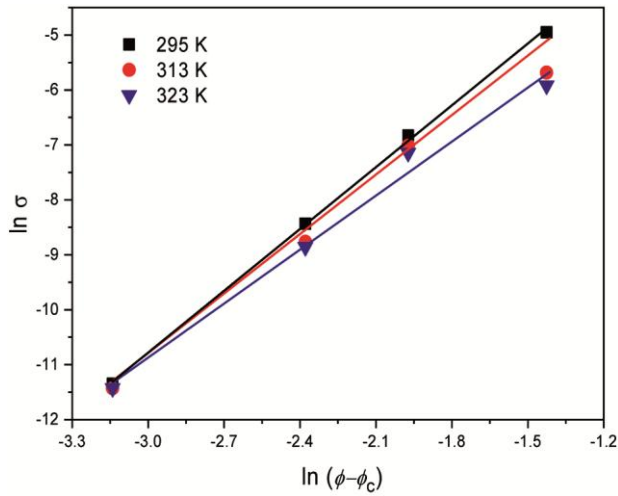


Fig. 4 — Log σ versus log $(\phi - \phi_c)$ at three temperatures 295 K, 313 K and 323 K for EPDM/HAF composites.

0.07 at 295, 313 and 323 K respectively. A slight temperature dependence of the exponent t was observed. The obtained values of t matched well with those reported by many other authors³². Additionally, the conductivity σ_0 was estimated from Fig. 4 as $\sim 2 \times 10^{-7} (\Omega \cdot cm)^{-1}$.

3.2.2 Temperature dependence of the conductivity

The conduction mechanisms in EPDM/HAF composites can be described by discussing the behavior of the electrical resistivity ρ (or conductivity σ) with the temperature T . Fig. 5 depicts the relationship between ρ and $1/T$ for the EPDM/HAF composites at various HAF carbon black contents, in the temperature range from 295 K up to 400 K. The resistivity has no fixed trend for all samples. This means that the resistivity depends on both temperature range and on the carbon black content. Thus, the resistivity of the EPDM/HAF composites can be divided into three categories according to the filler content of the samples. The first category included the behavior of low concentration sample (sample H30). The second category represented the medium concentration samples (samples H40 and H50). The third class described the behavior of the high concentration sample (sample H80).

(i) Low carbon black concentration range

This range was represented by sample H30. The resistivity increased by lowering down the temperature in the whole specified temperature range (Fig. 5). This was a typical insulator-like behavior. As the filler concentration was low enough, the distance between the aggregates became very large so that the carriers

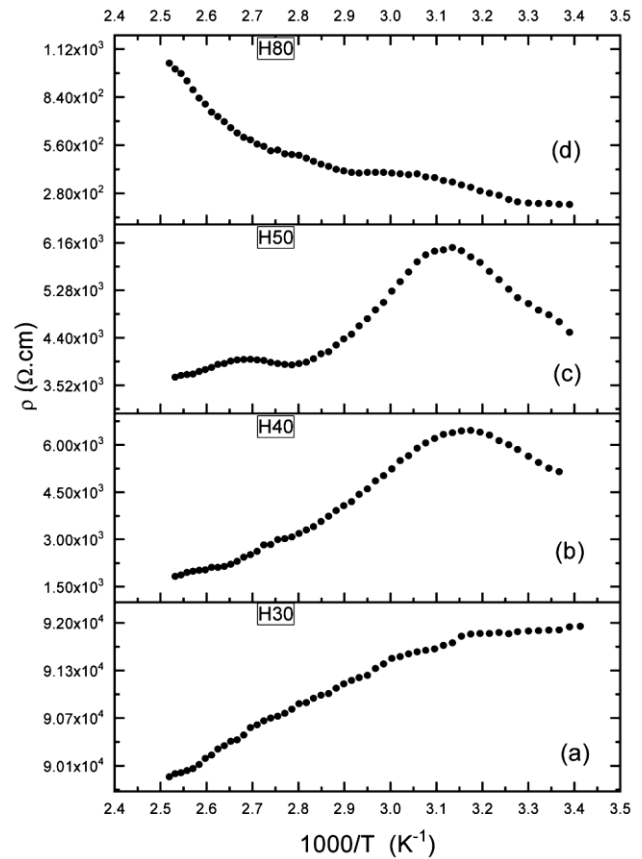


Fig. 5 — The electrical resistivity versus $1/T$ of EPDM/HAF composites at various HAF carbon black concentrations: (a) 30 phr, (b) 40 phr, (c) 50 phr and (d) 80 phr.

cannot jump easily between them. Moreover, in insulator-like systems, one would expect that the probability of transition of charge carriers between the formed aggregates is controlled by the temperature T . This transition probability decreases by lowering the temperature. Therefore, the continuous increase in ρ with the decrease of T can be understood. The conduction mechanism in this case may be assumed to be due to a thermal activation of charge carriers between the carbon energy states in the same aggregate. The activation energy of the charge carriers is calculated from the slope of the straight portion of $\ln \rho - 1/T$ plot. Fig. 6 shows such a graph for sample H30. It is clear that no constant activation energy can be detected through the whole range of temperature. For this particular sample, a possible hopping process may be suggested. It is obvious from Fig. 6 that a nearest-neighbor-hopping process of constant activation energy can be excluded. Now if a variable range hopping (VRH) mechanism was dominant, one would plot $\ln \rho$ versus $(\frac{1}{T})^{1/4}$ according to Mott's law³³

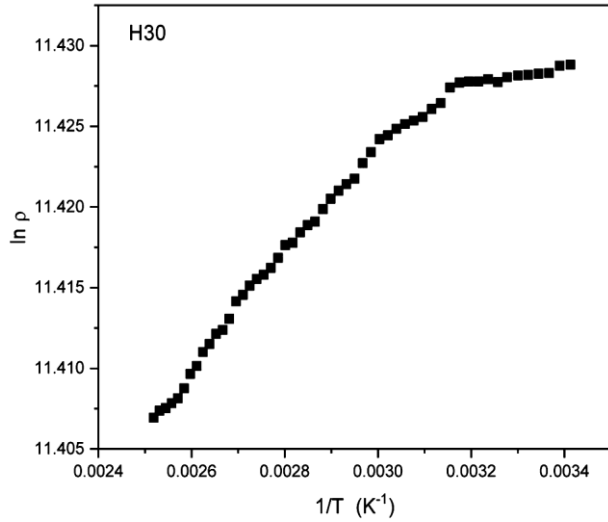


Fig. 6 — $\ln \rho$ versus $1/T$ of EPDM/HAF composites for sample H30.

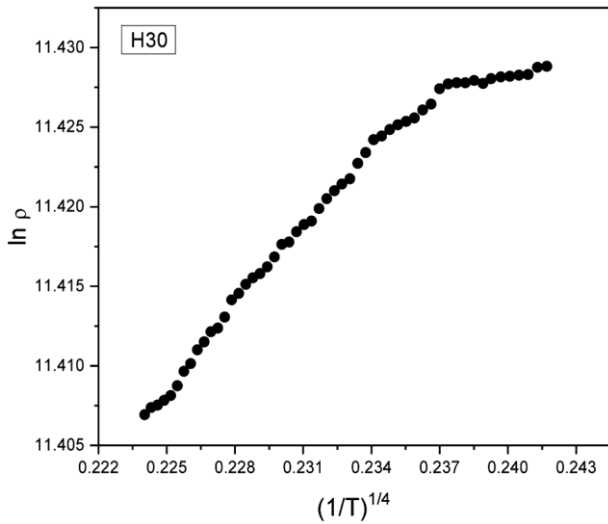


Fig. 7 — $\ln \rho$ versus $(1/T)^{1/4}$ of EPDM/HAF composites for sample H30.

$$\rho = \rho_o \exp \left[\left(\frac{T_o}{T} \right)^{1/4} \right] \quad \dots (3)$$

or $\ln \rho$ versus $\left(\frac{1}{T} \right)^{1/2}$ following Shklovskii and Efros law³⁴

$$\rho = \rho_o \exp \left[\left(\frac{T_o}{T} \right)^{1/2} \right] \quad \dots (4)$$

where T_o is a constant and the pre-exponential factor ρ_o is weakly temperature dependent. Figures 7 and 8 show such plots for sample H30. Inspection of Figures 7 and 8 revealed that neither of these suggestions can be followed.

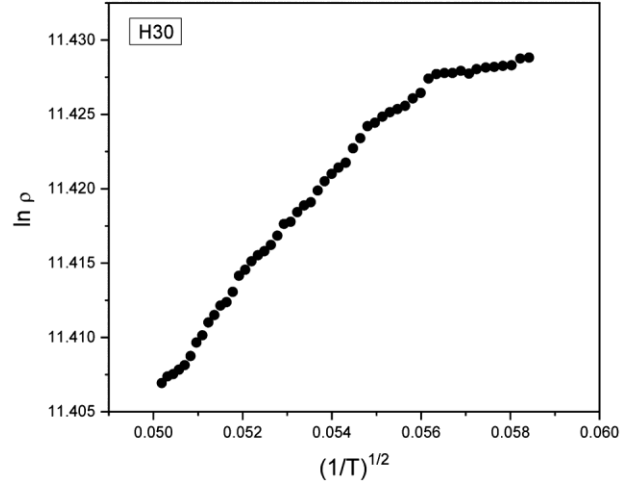


Fig. 8 — $\ln \rho$ versus $(1/T)^{1/2}$ of EPDM/HAF composites for sample H30.

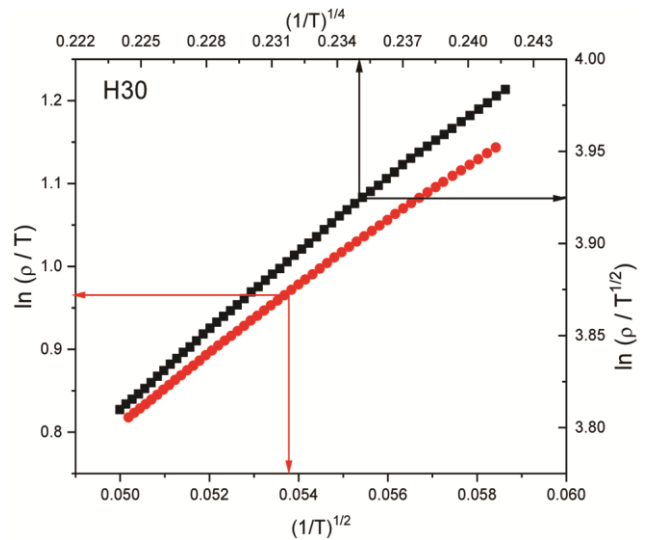


Fig. 9 — plots of $\ln(\rho/T^{1/2})$ versus $(1/T)^{1/4}$ and $\ln(\rho/T)$ versus $(1/T)^{1/2}$ for sample H30 of EPDM/HAF composites.

It was argued by Mansfield *et al.*³⁵ & Abboudy *et al.*³⁶ that one should consider the temperature dependence of the pre-exponential factor so that equation 3 takes the form;

$$\left(\frac{\rho}{T^{1/2}} \right) = \rho'_o \exp \left[\left(\frac{T_o}{T} \right)^{1/4} \right] \quad \dots (5)$$

and equation 4 becomes;

$$\left(\frac{\rho}{T} \right) = \rho'_o \exp \left[\left(\frac{T_o}{T} \right)^{1/2} \right] \quad \dots (6)$$

Thus, plots of $\ln(\rho/T^{1/2})$ versus $(1/T)^{1/4}$ and $\ln(\rho/T)$ versus $(1/T)^{1/2}$ were given in Fig. 9 for a comparison.

It was not quite clear whether $T^{1/4}$ law or $T^{1/2}$ law was followed. Further measurements at much wider temperature range were advised. As a general note one may assume that the present composite is approximated as an effective homogeneously disordered solid, thus the VRH model may be applied.

The $T^{1/4}$ and $T^{1/2}$ dependencies were observed previously in rubber filled with carbon black heterogeneous materials^{8,14}. In this case, thermal fluctuations of the Fermi level of electron states in NGPs, induce inter-NGP tunneling through the separating polymer barrier¹⁴. The FIT theory is used to interpret electronic transport in heterogeneous materials consisting of an insulating matrix and dispersed conducting inclusion⁸. It is necessary to point out that, the reduced form of the temperature dependence of the conductivity ($T^{-1/2}$ -dependence) is predicted both by FIT and Shklovskii-Efros' VRH. The physical concept is different; the VRH occurs in homogeneously disordered materials (such as amorphous semiconductors) by phonon-assisted-tunneling of electrons between localized states. On the other hand, FIT occurs for inhomogeneously disordered systems as electron states extend over the volume of each conducting grain and tuned to neighboring grains due to thermal fluctuation of Fermi level^{8,14}.

(ii) Medium carbon black concentrations

This range was represented by samples H40 and H50. The larger filler concentration the shorter distance between filler aggregates. Thus, the chance of carrier jumping between the aggregates became more probable. Overlapping of the carrier wave functions, then, can occur. The graphs of samples H40 and H50 showed an initial increase in ρ followed by a gradual decrease with the continuous reduction of T . Then a possible semiconductor-like behavior can be suggested for these samples. Two distinct conduction mechanisms, then, were observed. The initial increase of ρ with lowering down of T resembled an intrinsic behavior. The temperature dependence of ρ in this range can be represented by³⁷;

$$\rho = \rho_o \exp\left(\frac{E_a}{kT}\right) \quad \dots (7)$$

where k is the Boltzman constant and E_a is the carriers activation energy. Fig. 10 represents a plot of $\ln \rho$ versus $1/T$ for samples H40 and H50 in a temperature range from 400 K down to almost 320 K. The slope of the obtained straight lines gave the carriers activation energies. Estimated values of E_a

were 0.212 eV and 0.138 eV for samples H40 and H50, respectively. A sample of higher carbon black concentration had a lower value of E_a and this was expected.

The second region of the $(\rho-1/T)$ graph for H40 and H50 revealed a decrease in ρ with the further reduction of T below about 320 K. This was probably due to carrier- phonon scattering process. One then suggested that the conduction mechanism may follow an equation of the type³⁷;

$$\rho \propto T^n \quad \dots (8)$$

where n is a resistivity exponent. The relationship between $\ln \rho$ and $\ln T$, in the possible carrier-phonon scattering region, was plotted in Fig. 11 for samples

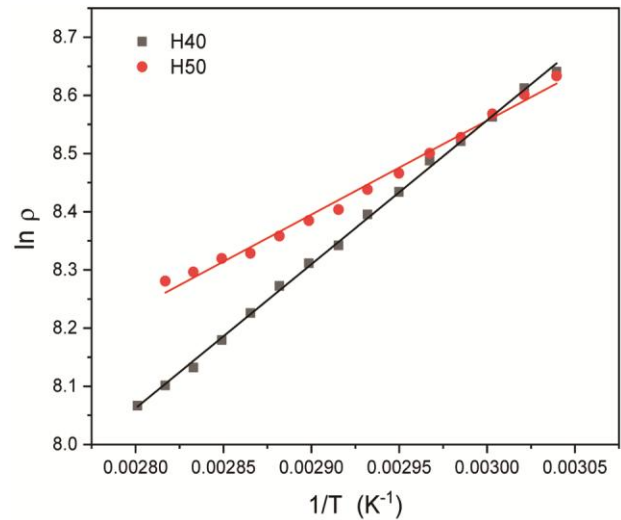


Fig. 10 — $\ln \rho$ versus $1/T$ for samples H40 and H50 of the EPDM/HAF composites.

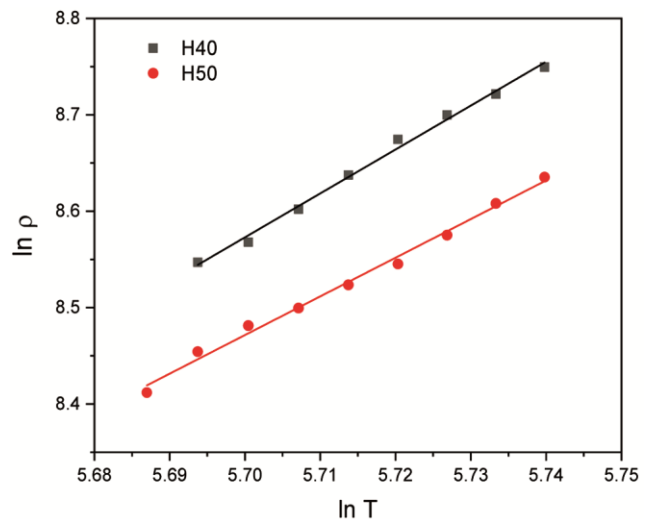


Fig. 11 — $\ln \rho$ versus $\ln T$ for samples H40 and H50 of the EPDM/HAF composites.

H40 and H50. The slopes of the straight lines lead to values of n as 4.55 ± 0.14 and 4.01 ± 0.13 for H40 and H50 respectively.

(iii) High carbon black concentrations

At high carbon black concentrations, which was represented by sample H80, the resistivity decreased continuously by lowering the temperature during the whole temperature range from 400 K down to 295 K. This may be ascribed as a metallic-like behavior. As noticed from SEM micrographs, at HAF content of 80 phr, big aggregates were formed. This enhances the electrical conduction as the charge carriers can move easily between these aggregates and consequently leads to an increase in the electrical conductivity. The material, hence, behaves like a metal. In this case, the dominant mechanism might be described by the carrier-phonon scattering or/and carrier-carrier scattering processes³⁷.

4 Conclusions

Samples of EPDM rubber loaded with HAF carbon black of 30, 40, 50, 80 and 100 phr were synthesized. The XRD data demonstrated the characteristic carbon black peaks corresponding to the (002) and (100) layers. SEM photographs evidenced the presence of carbon black aggregates inside the rubber. The existence of conductive carbon black filler in the rubber had a great effect on the electrical conductivity of the composites. At fixed temperature, a sudden increase of the conductivity was noticed above threshold filler content of volume fraction 0.16 vol %. The conductivity behavior with filler concentration was explained by the concepts of the percolation theory. The percolation exponent was found to vary slightly with temperature. The temperature dependence of the conductivity revealed that the conduction mechanisms were influenced by HAF carbon black concentrations. At low filler content (30 phr), the conductivity may be of a variable range hopping nature. Intermediate filling of carbon black (40 and 50 phr) resulted in a semiconductor-like behavior with two distinct conduction mechanisms. Higher filler contents (80 phr) might convert the composite to metallic-like material.

Acknowledgement

K. Alfaramawi wishes to thank the Deanship of Scientific Research at King Saud University, Saudi Arabia, for partially supporting this work through the research group project (RG-1436-030).

References

- 1 An J E & Jeong Y G, *Eur Polym J*, 49 (2013) 1322.
- 2 Alfaramawi K, *Mater Res Express*, 5 (2018) 066202.
- 3 Sandler J K W, Kirk J E, Kinloch I A, Shaffer M S P & Windle A H, *Polym*, 44 (2003) 5893.
- 4 Alfaramawi K, *Polym Bull*, 75 (2018) 5713.
- 5 Carpi F, De Rossi D, Kornbluh R, Pelrine R E & Sommerlarsen P, *Models and Applications of an Emerging Electroactive Polymer Technology*, (Elsevier Science), 2011.
- 6 Lawandy S N, Halim S F & Darwish N A, *Express Polym Lett*, 3 (2009) 152.
- 7 Stauffer D & Aharony A, *Introduction to percolation theory*, (Taylor and Francis, London) 1994.
- 8 Sheng P & Klafter J, *Phys Rev B*, 27 (1983) 2583.
- 9 Voet A, Whitten W N & Cook F R, *Kolloide Keitschrift Zeikhriji fur Polymerey*, 21 (1965) 39.
- 10 McCullough R L, *Compos Sci Technol*, 22 (1985) 3.
- 11 Scarisbrick R M, *J Phys D: Appl Phys*, 6 (1973) 2098.
- 12 Abd- El- Messieh S L, El Nashar D E, Younan A F & Abd- El- Nour K N, *KGK Rubberpoint*, 11 (2013) 36.
- 13 Reffae A S A, El Nashar D E, Abd- ElMessieh S L & Abd-El Nour K N, *Mater Des*, 30 (2009) 3760.
- 14 Kolonelou E, Loupou E, Klonos P A, Sakellis E, Valadorou D, Kyritsis A & Papathanassiou A N, *Polym*, 224 (2021) 123731.
- 15 Abou Z M M, *Eur Polym J*, 43 (2007) 4415.
- 16 Sajith T A, Praveen K M, Thomas S, Ahmad Z, Kalarikkal N, Dhanani C & Maria H J, *Prog Nucl Energ*, 141 (2021) 103940.
- 17 Azizi S, Momen G, Ouellet-Plamondon C & David E, *Polym Test*, 84 (2020) 106281.
- 18 Airinei A, Asandulesa M, Stelescu M D, Tudorachi N, Fifere N, Bele A & Musteata V, *Polym*, 13 (2021) 2555.
- 19 Mishra V, *IOP Conf. Series: Mater Sci Eng*, 1116 (2021) 012004.
- 20 Mahmood N Q, Marossy K & Baumli P, *Coll Polym Sci*, in press (2021).
- 21 Bazli L, Eskandarinezhad S, Kakur N, Ramachandran V, Bacigalupe A, Mansilla M & Escobar M, *J Compos Comp*, 3 (2021) 18.
- 22 Jha N, Sarkhel G & Mahapatra S P, *Mater Today Proc*, 45 (2021) 3850.
- 23 Paran S M R, Naderi G, Javadi F, Shemshadi R & Saeb M R, *Mater Today Commun*, 22 (2020) 100763.
- 24 Padhi S, Parida S, Sahoo P K, Naik B, Parida B N & Nayak N C, *Mater Today Proc*, 41 (2021) 211.
- 25 ASTM D3182-07 Rubber mixing; 2012.
- 26 Karasek L & Sumita M, *J Mater Sci*, 31 (1996) 281.
- 27 Ungar T, Gubicza J, Ribarik G & Pantea C Z T W, *Carbon*, 40 (2002) 929.
- 28 Biscoe J & Warren B E, *J Appl Phys*, 13 (1942) 364.
- 29 Singh A K, *Advanced X-ray Techniques in Research and Industry* (IOS Press, Amsterdam, The Netherland) 2005.
- 30 Vinayasree S, Soloman M A & Sunny V, *J Sci Technol*, 82 (2013) 69.
- 31 Janzen J, *J Appl Phys*, 46 (1975) 966.
- 32 De S K & White J R, *Short fiber-polymer composites* (Woodhead Publishing Limited, Cambridge, England) 1996.

- 33 Mott N F & Davis E A, *Electron Processes in Non-Crystalline Materials* (Oxford, Clarendon) 1979.
- 34 Shklovskii B I & Efros A L, *Electronic Properties of Doped Semiconductors* (Springer, Berlin) 1984.
- 35 Mansfield R, Abboudy S & Fozooni P, *Phil Mag*, 57 (1988) 777.
- 36 Abboudy S, Mansfield R & Fozooni P, *Proceedings of the international conference: Applications of high magnetic fields in semiconductor physics*, Springer-Verlag Series in Solid State Science, Edited by Landwehr G, 71 (1987) 518.
- 37 Kasap S, Koughia C & Ruda H E, 'Electrical Conduction in Metals and Semiconductors' in *Springer Handbook of Electronic and Photonic Materials*, edited by Kasap S & Capper P (Springer Handbooks. Springer, Cham) 2017.